

A new watermarking method based on Analytical Clifford Fourier Mellin Transform

Maroua Affes¹ Malek Sellami Meziou² and Faouzi Ghorbel¹

¹ CRISTAL Laboratory, GRIFT research group

Tunisia, Manouba

maroua.affes@ensi-uma.tn

malek.meziou@gmail.com

Faouzi.ghorbel@ensi.rn.tn

Abstract. Here, we intend to introduce a new Fourier Transform. The well-known Analytical Fourier Mellin Transform (AFMT) will be defined on Clifford Algebra in order to process colored images. The proposed Fourier Transform is called Clifford Analytical Fourier Mellin Transform (CAFMT). Its magnitude, same as AFMT modulus, is invariant against planar similarities, not only on gray level images but also on colored images. Using CAFMT magnitude, we propose a robust watermarking technique in the frequency domain.

Keywords: Analytical Fourier Mellin Transform, Clifford Transform, and robust watermarking method.

1 Introduction

Nowadays, many techniques are proposed to protect the intellectual property rights of multimedia data such as digital watermarking. It consists of embedding a mark into an input signal or its Fourier transform. Often, watermarking methods are categorized by processing domain and watermark signal type. In all cases, the following constraints must be considered: good visual fidelity and robustness of the watermark against common image processing geometric attacks are essential.

Digital image watermarking can be applied in either spatial domain or frequency domain or both of them. With the spatial watermarking methods, the image is directly manipulated to embed the mark in some pixels. However, the frequency watermarked methods decompose initially the image into frequencies coefficients and the embedding is done by changing the transform coefficients. Generally, the embedding process and extraction process have common steps and a same frequency transform. Applying spatial domain watermarking method is easier than the transform domain watermarking method [1]. But, the mark is simpler to detach from cover image by pixel-wise forgery attack. That's why, the frequency domain watermarking is mostly used than to spatial domain. Since, they give the mark higher robustness and offer resistance to image manipulations [2]. Also, they have a high level of imperceptibility. The transforms currently used are: Discrete Cosine Transform (DCT), Discrete Fourier Transform (DFT), Discrete Wavelet Transform, etc.

Authors in [3] present efficient method of watermarking using the DCT (Discret Cosinus Transform) magnitude. Ruanaidh and al. [4] suggest a robust watermarking technique based on the DFT (Discret Fourier Transform) phase. Pereira and Pun in [5] propose a robust watermarking algorithm using a new template integrated in image able to estimate the geometrical attacks and inverse it before extraction processes. The wavelet transform was usually used in image watermarking [6]. First, the original image is decomposed into multi subbands which present low and high frequency components. after that, the mark is embedded into some subbands.

In this article, we focus on the frequency watermarking techniques which is based on the Fourier transform. This transform allows researchers to extract features that are invariant to geometric transformations as rotation, translation and scaling. Several invariant descriptors have been proposed in the literature, we can cite, for example, the Generic Fourier Descriptors [7] and the Generalized Fourier Descriptors [8]. These descriptors are based on the discrete Fourier transform (DFT) which ensures the invariance of amplitude to translation. Also, other descriptors called the Mellin Analytic Fourier Descriptors have been introduced. They ensure the invariant to rotation and scale transformations by converting the image to polar or log-polar domain [9]. These descriptors form a complete family of invariants and have been used usually for grayscale images or in marginal treatment that consider each colorimetric plane separately.

To avoid this marginal treatment, Sangwine et al. [10] in 2000 proposed the "Quaternionic Color Fourier Transform". Based on this transform, Guo and Zhu [11] introduced the Quaternionic Fourier-Mellin Descriptors. In 2010, Batard et al. [12] proposed a more rigorous mathematical formulation of color transform, called the "Fourier Transform Clifford" and applicable directly to the color images. By analogy with the work done by Batard et al. [12], J. Mennesson [13] defined the "Fourier-Mellin Clifford Descriptors" that are based both on the Fourier transform Mellin and Clifford algebra. These descriptors appeared as a promising tool in the processing of color images only for shape recognition. Given the important proprieties of these descriptors, we propose to integrate them into a color watermarking system.

In this paper, we give an overview of some Fourier transforms used in watermarking technology. Then we will present our new method which is based on Analytical Clifford Fourier Mellin Transform. Experimental results will be presented in the section 4. We will eventually conclude and suggest some possible perspectives for future work.

2 New watermarking method based on ACFMT

In this section, we will introduce the Analytical Clifford Fourier Mellin transform. This transform will be used later to propose a robust watermarking algorithm against geometric attacks.

Let f denote a function of a grayscale image, represented with polar coordinates (r and θ) defined over a compact set of $\mathbb{R}_+^* \times S^1$ [14,15]. The Fourier Mellin Transform of f is given by:

$$M_f(k, v) = \frac{1}{2} \int_0^\infty \int_0^{2\pi} f(r, \theta) \cdot r^{iv} \cdot e^{-ik\theta} \cdot \frac{dr}{r} \cdot d\theta, \forall (k, v) \in Z \times R \quad (1)$$

f is assumed to be assumable over $\mathbb{R}_+^* \times S^1$ under the measure $\frac{dr}{r} \cdot d\theta$ i.e

$$\int_0^\infty \int_0^{2\pi} |f(r, \theta) \cdot r^{-iv} \cdot e^{-ik\theta}| \cdot \frac{dr}{r} \cdot d\theta = \int_0^\infty \int_0^{2\pi} f(r, \theta) \cdot dr \cdot d\theta < \infty \quad (2)$$

This hypothesis is not justified over $\mathbb{R}_+^* \times S^1$. Indeed, the integral diverges near the origin as $f(0, \theta)$ is generally non-zero. A rigorous approach has been introduced to tackle the divergence problem, Ghorbel in [16] suggested computing the FMT of $f_\sigma = r^\sigma f(r, \theta)$ instead of $f(r, \theta)$ where σ is a fixed and strictly positive real number. The Analytical Fourier Mellin transform has the following expression:

$$M_{f_\sigma}(k, v) = \frac{1}{2} \int_0^\infty \int_0^{2\pi} f(r, \theta) \cdot r^{\sigma-iv} \cdot e^{-ik\theta} \cdot \frac{dr}{r} \cdot d\theta, \forall (k, v) \in Z \times R \quad (3)$$

The AFMT presents enormous benefits but it can be computed only on gray level images. Quaternion transform and Clifford transform have been proposed to overcome this problem. First, the QFT is defined by replacing the imaginary complex i in the exponential of the Fourier transform by a pure and unitary quaternion μ belongs to \mathbb{H}_1 . A color image is then considered as a function \mathbb{R}^2 on $\mathbb{R}_{4,0}$:

$$f(x) = r(x)i + v(x)j + b(x)k \quad (4)$$

After that, a pixel of a color image f can be extended as follows:

$$f(x) = r(x)e_1 + v(x)e_2 + b(x)e_3 + 0e_4 \quad (5)$$

Where $x = (x_1, x_2)$ and r, v and b are respectively the red, green and blue channels pixel with coordinates (x_1, x_2) .

The CFT generalizes the Color QFT [11]. The CFT is parameterized by a unit vector B whose expression is as follows:

$$\hat{f}_B(u) = \int_{R_2} e^{\frac{1}{2}\langle u, x \rangle B} e^{\frac{1}{2}\langle u, x \rangle I_4 B} f(x) e^{-\frac{1}{2}\langle u, x \rangle B} e^{-\frac{1}{2}\langle u, x \rangle I_4 B} dx \quad (6)$$

Where $\langle \rangle$ represents the scalar product, I_4 is the scalar pseudo of $\mathbb{R}_{4,0}$ and B is its unit bi-vector. Within the Clifford algebras, a vector can be decomposed into a parallel part and an orthogonal part relative to a bivector B . The above equation can be rewritten as follows by this decomposition [13]:

$$\hat{f}_B(u) = \hat{f}_{\parallel B}(u) + \hat{f}_{\perp B}(u) \quad (7)$$

Where $\hat{f}_{\parallel B}(u) = \int_{R_2} f_{\parallel B}(x) e^{-\langle u, x \rangle B} dx$ and $\hat{f}_{\perp B}(u) = \int_{R_2} f_{\perp B}(x) e^{-\langle u, x \rangle I_4 B} dx$

In order to combine the CFT with MFT, J. Mennesson in [13] proposed the Clifford Fourier Mellin transform.

$$\hat{f}_B(m, n) = \int_0^\infty \int_0^{2\pi} r^{m-1} e^{\frac{1}{2}n\theta(B+I_4B)} f(r, \theta) e^{-\frac{1}{2}n\theta(B+I_4B)} dr \cdot d\theta \quad (8)$$

This transform is divergent near the origin. We propose to compute the Analytical CFMT with the log-polar sampling ($q = \ln(r)$). The Analytical CFMT that we note ACFMT is defined by the following expression:

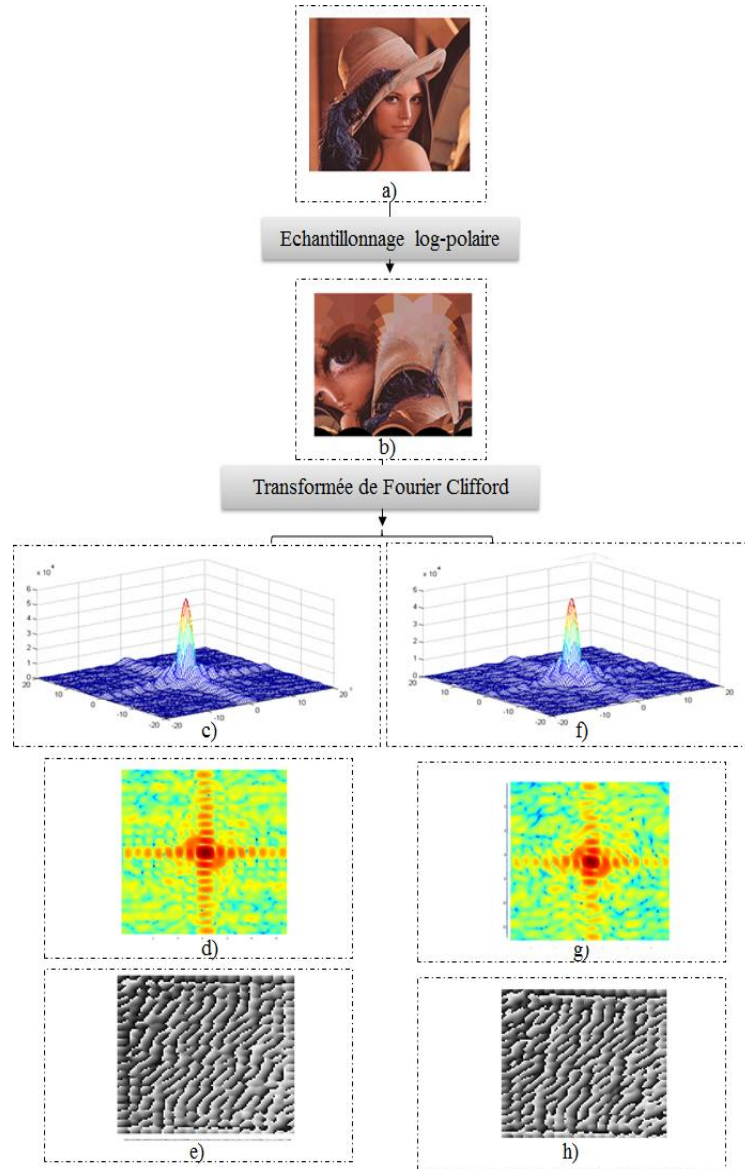


Fig. 1: The visualization of the Analytic Clifford Fourier Mellin transform:

a) Original image with size of 512x512 b) Log-polar mapping of (a) image c) 3D spectrum representation of the CFT (parallel part) d) 2D spectrum representation of the CFT (parallel part) e) Phase representation of the CFT (parallel part) f) 3D spectrum representation of the CFT (orthogonal part) g) 2D spectrum representation of the CFT (orthogonal part) h) Phase representation of the CFT (orthogonal part)

$$\hat{f}_B(m, n) = \int_0^\infty \int_0^{2\pi} e^{q\sigma+m-1} e^{\frac{1}{2}n\theta(B+I_4B)} f(e^q, \theta) e^{-\frac{1}{2}n\theta(B+I_4B)} dq d\theta \quad (9)$$

Where I_4 is the scalar pseudo of $\mathbb{R}_{4,0}$ and B is its unit bi-vector. And $f(e^q, \theta)$ represents the log-polar transform of the image f . To simplify the computational complexity, we use the fast approximation [14]. Figure 1 shows the steps to estimate the Fourier Transform Mellin Clifford Analytics and display the results of each step.

3 The proposed algorithm

In this section, we will present our proposed method which done in frequency domain. We use the CFT as a Fourier transform applicable directly on color image. With the CFT, we avoid a marginal treatment and we ensure that there is not appearance of false color. Besides, the mark will be more robust.

We will use the decomposition of the CFT in order to embed the mark. In [17], we set up a small experiment to choose the embedding plane; we embed the mark W in three different locations: the parallel part, in the orthogonal part and in both of them. The results demonstrate that the emending in the parallel part deteriorate less the perceptual image quality.

Also, to make our method more robust, we used the local Harris features which can synchronize the embedded regions and the extracted regions. They provide a potential solution for watermarking to improve the robustness [18]. In fact, the interest points present a center of circular regions which contains the mark. These same regions may be identified in extraction process even after geometric distortions.

3.1 Embedding process

In Figure 2, we present the general diagram of our watermarking method. The embedding process has the following steps:

- Transform the image to gray scale image to detect the interest points.
- Generate some non-overlapped interest regions.
- Generate a bitmap, denoted ξ , which contains "1" if the block $B(i)$ of $\hat{f}_{\parallel B}$ is valid i.e the block has a bit of the watermark. The validity condition is compute by the next steps:
 - ACFMT is applied to each selected block
 - Two mid-frequency coefficients are selected, $|Q(k_i, l_j)|$ and $|Q(k_n, l_m)|$:
 If $|Q(k_i, l_j)| > |Q(k_n, l_m)| + p$,
 So $\xi(i) \leftarrow 1$; the Block $B(i)$ is valid.
 Else
 $\xi(i) \leftarrow 0$.
 End if

Where p is a marginal noise, in the experiment $p = 0.5$.

- Generate the mark W , $\{W_i, i = 0 \dots N\}$. Its size is the number of "1" in the map. In order to overcome the corruption of the mark due to attacks, we use the Hamming code as an error correcting codes. So, the watermark is divided

into some words, each word contains 4 bits. The Hamming code is then applied to each word to generate (7-4) single bit error correcting code. The use of error-correction codes ensures a better-quality signal at the receiver [19].

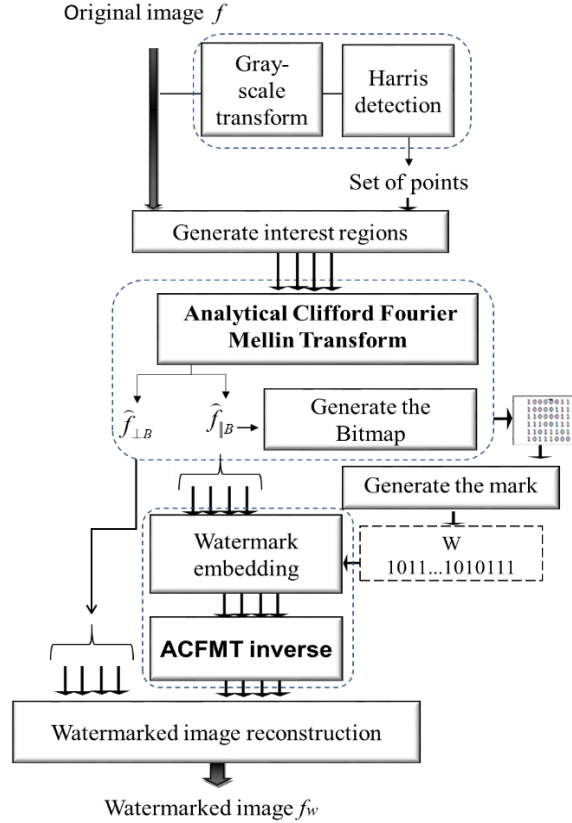


Fig. 2 : Embedding process

- Embed the mark in valid regions, each region will contain one bit. To do that, we modified $|Q(k_i, l_j)|$ and $|Q(k_n, l_m)|$ and denoted the watermarked coefficients by $|Q'(k_i, l_j)|$ and $|Q'(k_n, l_m)|$, we apply the fellow steps:
 If $\xi(i) = 1$
 Apply the ACFMT;
 If $W(i) = 1$ So
 $|Q'(k_i, l_j)| = |Q(k_n, l_m)|$ and $|Q'(k_n, l_m)| = |Q(k_i, l_j)|$; (we permute $|Q(k_i, l_j)|$ and $|Q(k_n, l_m)|$)
 Else
 $|Q'(k_i, l_j)| = |Q(k_i, l_j)|$ and $|Q'(k_n, l_m)| = |Q(k_n, l_m)|$;
 Endif
 Apply the Inverse of ACFMT on each block.
 Else

- Pass to the next region;
- Endif
- The watermarked image f_w is then obtained by combining the watermarked blocks with the others blocks.

3.2 Extraction process

The first steps of the extraction process are the same steps to those in embedding process. With the presence of the secret key and the map ξ , we can specify which blocks are watermarked. So, when $\xi(i) = 1$, we transform $B(i)$ to ACFM domain. The watermark is extracted by the following equation:

$$W' = \begin{cases} 1, & |Q'(k_n, l_m)| > |Q'(k_i, l_j)| \\ 0, & |Q'(k_n, l_m)| < |Q'(k_i, l_j)| \end{cases} \quad (10)$$

4 Experimental results

For all tests, we chose $|Q(k_i=3, l_j=2)|$ and $|Q(k_n=1, l_m=4)|$ as two mid-frequency coefficients of ACFMT. They have been modified to carry one-bit watermark in each region.

We used the PSNR (Peak Signal Noise Ratio) to measure imperceptibility of the mark. Figure 3 and 4 show the obtained result after the insertion of the mark in the parallel plane.

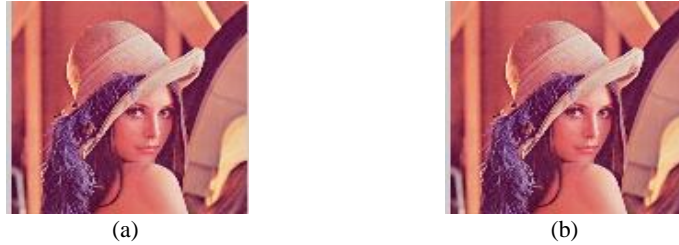


Fig. 3 : Visual quality experiment (a) originale image, (b) watermarked image where PSNR = 38.44 dB



Fig. 4 : Visual quality experiment (a) originale image (reference 6106), (b) watermarked image where PSNR = 47.55 dB

The value of the PSNR is depending on the number of interest regions modified. In fact, it decreases when the size of the mark increases.

To evaluate the robustness of the proposed algorithm, we compute the Bit Error Rate. It presents the ratio between the numbers of incorrect bits transmitted to the total number of bits. The following table describes the error rate of mark estimation after some attacks on the image "Lena" and some images taken from the BSD300 set (The Berkeley Segmentation Dataset).

Table 1. Error rate after some geometric attacks applied on "Lena" image.

Image reference / Attacks	Lena	61060	46076	78004	22090	8068	10081	15011	28083	35049
Rotation 1°	0,3	0	0	0,1	0,1	0	0,1	0,1	0	0
Rotation 5°	0.2	0.2	0	0.3	0.2	0	0	0	0.2	0
Rotation 10°	0.3	0.3	0	0.1	0.1	0.1	0	0	0	0.2
Translation 1 (5,5)	0	0	0	0	0	0	0	0.2	0	0
Translation 2 (1,3)	0	0	0	0	0	0.1	0	0	0.1	0
Scaling 0,7	0.3	0	0.1	0.2	0.1	0.1	0.2	0	0	0.1
Scaling 0,9	0.2	0	0.1	0.2	0	0	0	0.3	0	0
Scaling 1,1	0	0	0	0.2	0.1	1	0	0	0	0.2

The proposed method is robust since the amplitude of the Fourier transform is invariant against translation and scaling. Also, it is robust against rotation since the insertion takes place after log-polar mapping.

The zero value of BER indicates that the mark extracted correctly. However, the higher value of BER is 0.3 which indicates that there is a fail in detection process. This fail comes from the fact that the set of points changes after geometric attacks.

5 Conclusion and perspectives

In this paper, we introduced a new method of invisible watermarking based on ACFMT. The proposed algorithm is robust against geometric attacks because we synchronize the mark with the image content by embedding the mark in interest regions. The mark is imperceptible as it is inserted into the parallel part $\hat{f}_{\parallel B}$ of the Clifford Transform. The BER values showed that our scheme is effective in watermark recovering. But, its payload depends on the number of valid interest regions

Future work will aim to extend it to enhance the robustness and to ensure that the mark can be extracted fairly accurately. Also, we will study the robustness against compression attacks.

References

1. Mishra, A., Jain, A., Narwaria, M., & Agarwal, C. (2011). An experimental study into objective quality assessment of watermarked images. *International Journal of Image Processing (IJIP)*, 5(2), 199.
2. Potdar, V. M., Han, S., & Chang, E. (2005, August). A survey of digital image watermarking techniques. In *Industrial Informatics, 2005. INDIN'05. 2005 3rd IEEE International Conference on* (pp. 709-716). IEEE.
3. Burgett, S., Koch, E., & Zhao, J. (1998). Copyright labeling of digitized image data. *IEEE Communications Magazine*, 36(3), 94-100.
4. Ruanaidh, J. J. K. O., Dowling, W. J., & Boland, F. M. (1996, September). Phase watermarking of digital images. In *Image Processing, 1996. Proceedings., International Conference on* (Vol. 3, pp. 239-242). IEEE.
5. Pereira, S., & Pun, T. (2000). Robust template matching for affine resistant image watermarks. *IEEE transactions on image Processing*, 9(6), 1123-1129.
6. Kundur, D., & Hatzinakos, D. (1997, October). A robust digital image watermarking method using wavelet-based fusion. In *Image Processing, 1997. Proceedings., International Conference on* (Vol. 1, pp. 544-547). IEEE.
7. Zhang, D., & Lu, G. (2002). Shape-based image retrieval using generic Fourier descriptor. *Signal Processing: Image Communication*, 17(10), 825-848.
8. Smach, F., Lemaître, C., Gauthier, J. P., Miteran, J., & Atri, M. (2008). Generalized Fourier descriptors with applications to objects recognition in SVM context. *Journal of mathematical imaging and Vision*, 30(1), 43-71.
9. Derrode, S., & Ghorbel, F. (2001). Robust and efficient Fourier–Mellin transform approximations for gray-level image reconstruction and complete invariant description. *Computer Vision and Image Understanding*, 83(1), 57-78.
10. Sangwine, S. J., Ell, T. A., Blackledge, J. M., & Turner, M. J. (2000). The discrete Fourier transform of a colour image. *Image Processing II Mathematical Methods, Algorithms and Applications*, 430-441.
11. Guo, L. Q., & Zhu, M. (2011). Quaternion Fourier–Mellin moments for color images. *Pattern Recognition*, 44(2), 187-195.
12. T. Batard, M. Berthier & C. Saint-Jean (2010). Clifford Fourier Transform for Color Image Processing. In E. Bayro-Corrochano & G. Scheuermann, éditeurs, *Geometric Algebra Computing in Engineering and Computer Science*, chapitre 8, pages 135–161. Springer Verlag. 5, 11, 12, 17, 18, 49, 51, 61, 63, 87, 108, 123, 124
13. Mennesson, J., Saint-Jean, C., & Mascarilla, L. (2014). Color Fourier–Mellin descriptors for image recognition. *Pattern Recognition Letters*, 40, 27-35.
14. Derrode, S. (1999). Représentation de formes planes à niveaux de gris par différentes approximations de Fourier–Mellin analytique en vue d'indexation de bases d'images (Doctoral dissertation, Rennes 1).
15. Ghorbel, F. (1993). Application de la transformée de Fourier généralisée au problème de l'invariance en reconnaissance de formes a niveaux de gris. In *14° Colloque sur le traitement du signal et des images, FRA, 1993. GRETSI, Groupe d'Etudes du Traitement du Signal et des Images*.

16. Ghorbel, F. (1994). A complete invariant description for gray-level images by the harmonic analysis approach. *Pattern recognition letters*, 15(10), 1043-1051.
17. Affes, M., Meziou, M. S., & Ghorbel, F. (2016, October). Robust Color Watermarking Method Based on Clifford Transform. In *International Conference on Advanced Concepts for Intelligent Vision Systems* (pp. 453-464). Springer International Publishing.
18. Papakostas, G. A., Tsougenis, E. D., Koulouriotis, D. E., & Tourassis, V. D. (2011). On the robustness of Harris detector in image watermarking attacks. *Optics Communications*, 284(19), 4394-4407.
19. MacWilliams, F. J., & Sloane, N. J. A. (1977). *The theory of error-correcting codes*. Elsevier.